ASIAN JOURNAL OF CIVIL ENGINEERING (BUILDING AND HOUSING) VOL. 7, NO. 1 (2006)
PAGES 13-26

CYCLIC BEHAVIOUR OF STEEL BRACED FRAMES HAVING SHEAR PANEL SYSTEM

S.M. Zahrai*[a] and A. Moslehi Tabar[b]
Deptartment of Civil Engeneering, University of Tehran,
P.O. Box 11365-4563, Tehran, Iran
Deptartment of Civil Engeneering, Amirkabir University of Technology, Tehran, Iran

ABSTRACT

Seismic resisting structures are expected to maintain adequate stiffness during frequent but moderate excitations on one hand, and to dissipate a large amount of energy under damaging earthquakes on the other hand. In this paper, a relatively new seismic resisting structural system, which satisfies stiffness and energy dissipation requirements simultaneously, is numerically investigated using nonlinear finite element analysis procedure. In this system, earthquake energy is dissipated through large inelastic deformation occurred within a shear panel. The shear panel acts as a ductile link beam connecting braces to the floor beam. This paper aims to find out key issues influencing cyclic behaviour of frames braced by Shear Panel System (SPS), like Cross-sectional properties of SPS and link length. The results indicate that shear panel length significantly affects cyclic performance of this system. Use of shorter links results in more stiffness and at the same time more stable hysteretic behaviour and energy dissipation capacity. Finally, the paper presents a mathematical model to evaluate lateral stiffness of braced frames braced having SPS.

Keywords: shear panel, eccentrically braced frames, inelastic deformation, earthquake, energy dissipation

1. INTRODUCTION

In seismic regions, properly designed and constructed structures are expected to maintain adequate stiffness during frequent but moderate excitations on one hand, and to dissipate a large amount of energy under damaging earthquake on the other hand. The conventional framing systems, i.e., concentrically braced frames, and moment frames are not able to satisfy stiffness and ductility requirements concurently. The concentrically braced frames usually possess high stiffness, but poor ductility owing to the buckling of the compression braces [1]. On the contrary, the steel moment frames are supposed to show acceptable ductility and energy dissipation capacity through flexural yielding in beams, while their

* Email-address of the corresponding author: mzahrai@ut.ac.ir

stiffness is limited. However, the 1994 Northridge and 1995 Kobe earthquakes revealed serious damages to the conventional steel moment frames [2-5]. A combination of these two systems can make a balance between requirements concerning stiffness and energy dissipation capacity.

To promote energy dissipation capability of a steel framed structure, Roeder and Popov [6] proposed Eccentrically Braced Frame (EBF) system in which the brace is placed eccentrically to the beam-to-column joint. High amount of energy can be dissipated by this system provided that the eccentricity is properly chosen. The EBF system suffers from some major drawbacks. For example, the energy dissipation capacity is provided by the shear links that are the integral parts of the beam elements, leading to serious damage to floor beam after a severe earthquake. Their repair may be difficult and expensive. In addition, since the floor beams are mostly of heavy sections, the braces must be proportionally strong in order to be able to activate the shear link.

In order to overcome the deficiencies with EBF system, Aristazabal-Ochoa [7] has proposed a new methodology. In this method the input energy is dissipated by a disposable shear link so-called disposable knee braced frame (DKBF). In this system, all the yielding concentrates within the shear link, and no serious damage is likely to take place in the main structure. Since the shear link is removable, repairing after earthquake becomes much easier. Balendra et al. [8,9] and Sam et al. [10] re-examined the KBF system and proposed modifications to control buckling of diagonal braces.

In this paper one of the most effective braced frame systems through which a high level of energy dissipation capacity may be attained is investigated. The system comprises an inverted-V-bracing framed to the floor beam through a shear panel. This system is well known as inverted-Y-bracing system in AISC s*eismic provisions* [11]. The shear panel is the energy-dissipating zone and may be a disposable element. The shear panel system (SPS) is more efficient and more practical in comparison with KBF system. Zahrai and Bruneau [12,13] have analytically and experimentally examined the efficiency of the SPS among other ductile devices installed in end-diaphragms of steel slab-on-girder bridges to modify their seismic response.

This study aims to find out key issues influencing cyclic behaviour of frames braced by SPS. These issues are including: beam-to-column connection type, cross-sectional properties of SPS, link length, brace slenderness, and web stiffener. To this end, a number of single story-single bay frames are numerically analyzed using nonlinear finite element procedure. The results indicate that shear panel length significantly affects cyclic performance of this system. Use of shorter links leads to more stiffness and more energy dissipation capacity at the same time.

2. PARAMETRIC STUDY

A parametric numerical study was conducted on a series of steel frames braced by shear panel system to investigate their cyclic behaviour. Six single story-single bay frames with the general configuration shown in Figure 1 were employed. In each specimen the beam was laterally supported in every 75cm along its length. Experimental investigations [12,13] show that since the floor beam is adequately protected against lateral deformation and the shear panel is relatively short, lateral deformation is not likely to occur at the shear panel. Accordingly, no extra lateral support is provided at the shear panel of the frames. The specimens were selected so that the effects of some major issues influencing the cyclic performance of this type of braced frames can be determined. These issues are including: beam-to-column connection type, cross-sectional properties of SPS, link length, brace slenderness, and web stiffener.

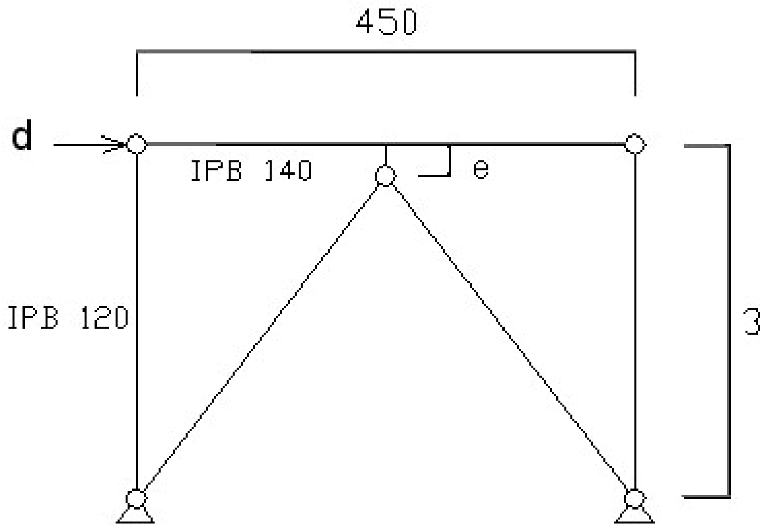

Figure 1. General configuration of specimens (applying lateral displacement, d, to frame)

3. DESIGN OF SPECIMENS

Since the design of a single story-single bay frame under actual loading generally results in small dimensions for the frame members, in each specimen the SPS was pre-selected and the other members including: columns, beam, and braces, were proportioned based on the SPS shear strength. The specimens were designed according to AISC s*eismic provisions* [11]. Specifications of the specimens are given in Table 1.

Based on AISC s*eismic provisions* [11], the required shear strength of the link (SPS), V_u, shall not exceed the design shear strength of the link ϕV_n, where:

V_n = nominal shear strength of the link, equal to the lesser of V_p or $2M_p/e$,

$V_p = 0.60F_y(d-2t_f)t_w$,

$\phi = 0.90$, and e, F_y, d, t_f, and t_w are link length, specified minimum yield stress of the steel, link depth, flange, and web thickness of link, respectively.

The design shear strength for each SPS is noted in Table 2.

Table 1. Specifications of specimens in analytical models

Spec.	Beam-to-column Connection Type	Braces	SPS	e* (cm)	Web stiffeners
SPS1	Rigid	2UNP100	IPE160	37	A pair at mid-height
SPS2	Pinned	2UNP100	IPE160	37	A pair at mid-height
SPS3	Pinned	2UNP100	IPE160	27	A pair at mid-height
SPS4	Pinned	2UNP60	IPE160	27	A pair at mid-height
SPS5	Pinned	2UNP80	IPE140	27	A pair at mid-height
SPS6	Pinned	2UNP80	IPE140	27	With no stiffeners

*** Eccentricity (e) is measured from the floor beam centreline. The net length of link equals the eccentricity less half of the beam depth.**

Table 2. Design shear strength of various SPs

Spec.	V_p (ton)	$2M_p/e$ (ton)	φV_n (ton)
SPS1	10.45	15.40	9.40
SPS2	10.45	15.40	9.40
SPS3	10.45	21.11	9.40
SPS4	10.45	21.11	9.40
SPS5	8.54	15.26	7.69
SPS6	8.54	15.26	7.69

4. FINITE ELEMENT ANALYSIS

4.1 Numerical modelling

The ANSYS finite element software [14] was utilized to model the specimens for large-deformation nonlinear analysis. The shear panel and a portion of the beam near it, which were expected to behave inelastically, were modeled using a quadrilateral 4-node shell element (SHELL43 in ANSYS) with plasticity, large deflection, and large strain capability. This element has six degrees of freedom per node: translations in x, y, z directions, and rotations about x, y, z axes. The element BEAM24, which is a 2D inelastic beam element, was employed to model the columns, braces, and the remaining portion of the beam. The shell elements were connected to the beam elements using rigid interface elements to satisfy continuity conditions. Figure 2 shows a typical finite element meshing used in this study. Nonlinear material was assigned to the all segments even though it was expected that nonlinear deformations were mostly accommodated around the shear panel. The plasticity model was based on the von Mises yielding criteria and its associated flow rule. The fundamental assumptions made to idealize steel mechanical properties were included: Young's modulus $=2.1\times10^6\,\mathrm{kg/cm^2}$, Poisson's ratio =0.3, yield stress $=2400\,\mathrm{kg/cm^2}$, ultimate tensile strength $=3700\,\mathrm{kg/cm^2}$, and tangent modulus = Young's modulus / 100.

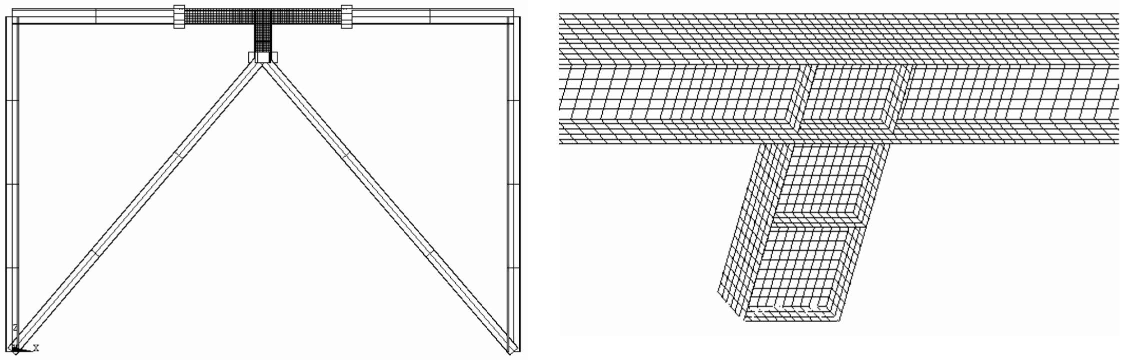

(a) (b)

Figure 2. Typical finite element model of specimens: (a) general model, (b) meshing of shear panel and regions near it

4. 2 Loading and analysis procedure

Each frame was loaded on its top by imposing the same cyclic displacements as proposed by AISC s*eismic provisions* [11], see Figure 3. Cyclic nonlinear analyses of the specimens were performed using Riks method. In this method, buckling mode shapes of the model, computed in a separate buckling analysis, are implemented to perturb the original perfect geometry of the model. Then, the obtained imperfect model is analyzed to take local and lateral buckling into account.

5. NUMERICAL RESULTS

5.1 Hysteretic response of specimens

The specimens were loaded up to five times the drift corresponding to yielding, except the specimen SPS4. In this specimen, the computation time highly increased due to the buckling of the braces and the analysis was therefore terminated. Lateral force-drift hysteretic responses of the specimens are illustrated in Figure 4. As observed in this figure, all the specimens possess stable and expanding hysteretic loops with no deterioration in stiffness and load-carrying capacity.

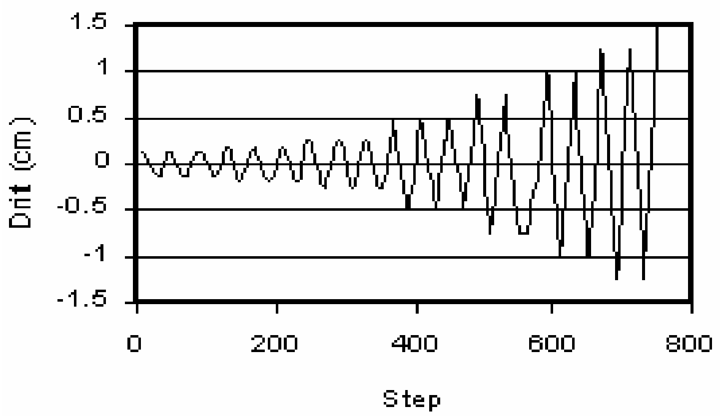

Figure 3. Lateral loading procedure imposed to the models

The effect of beam-to-column connection on the cyclic performance of the frames braced by the SPS may be interpreted by comparing Figs. 4(a) and 4(b). The specimens SPS1 and SPS2 are the same except that the beam is rigidly connected to the columns in SPS1 while in the frame SPS2, the simple connections are used. Figs. 4(a) and 4(b) indicate that the frame SPS1 with rigid connections reached more load-carrying capacity. Indeed, the shear panel of SPS1 was yielded later as compared with that of SPS2. In addition, the hysteretic loops of the frame SPS1 grew up with steeper slope in the post-yielding domain. These discrepancies have arisen from the interaction between the shear panel and the moment frame existing in the specimen SPS1. Since, the moment frame remained elastic during the loading, it could significantly affects performance of the specimen SPS1, especially after the shear panel had been yielded.

However, if a shorter link is used as the shear panel, the adverse effect of simple connections is reduced to some extent. For instance, the specimen SPS3, having the beam simply framed to the columns, shows the same hysteretic response as the frame SPS1 which has rigid connections. In essence, the shorter link makes frame stiffer in both elastic and plastic stages, and can compensate the stiffness developed by the moment frame. Consequently, if the link length is well selected, the need for moment beam-to-column connections may be reduced, at least for low-rise buildings. Furthermore, the behaviour of shorter links is mostly dominated by shear stress, resulting in a stable hysteretic response with a high energy dissipation capability, while in longer links, the normal stress due to the bending becomes a major concern, rising the fracture potential at the link-to-beam interface, and decreasing the efficiency of the shear panel [15]. This fact can be concluded by comparing the hysteretic behaviour of the specimens SPS2 and SPS3, see Figs. 4(b), and 4(c).

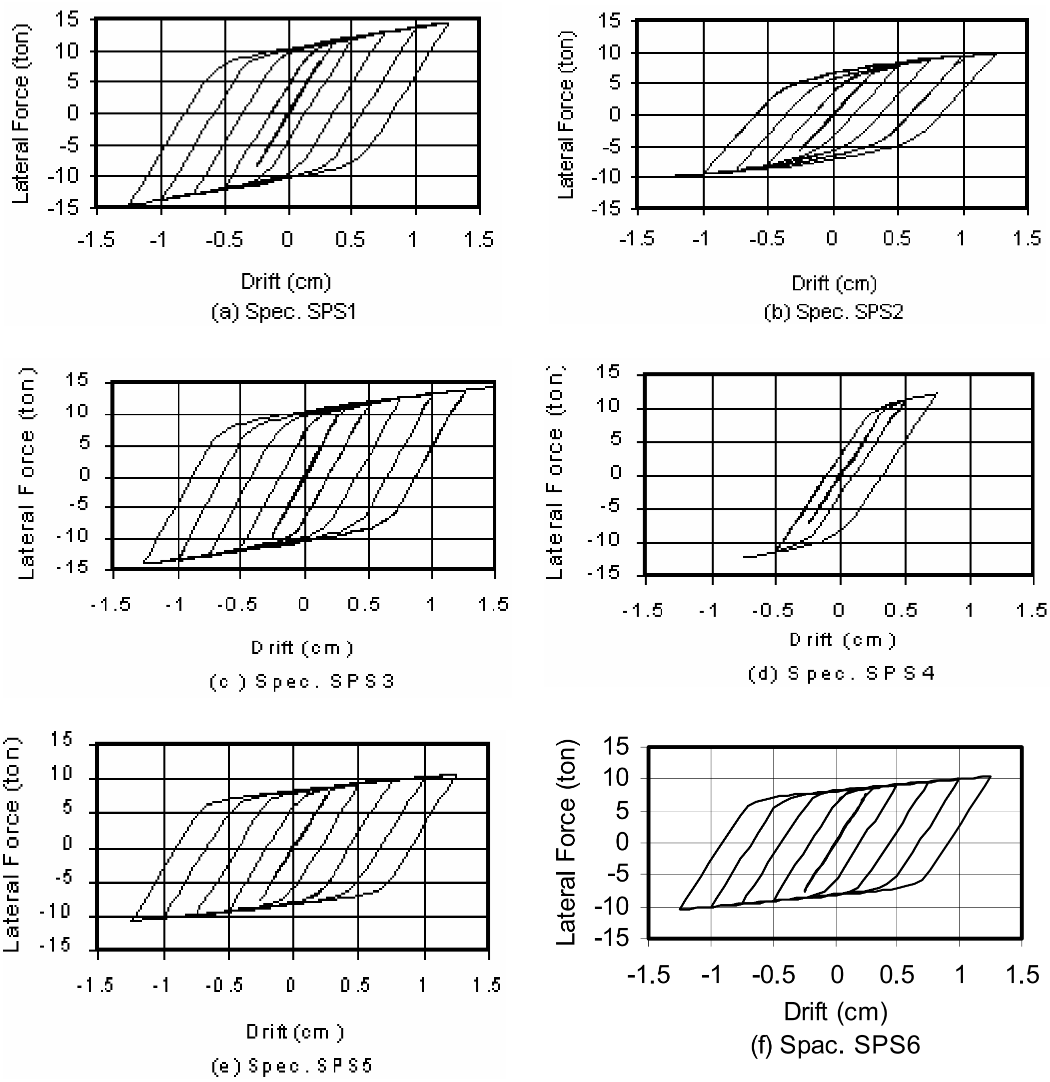

Figure 4. Lateral force-drift hysteretic response

The braces of the specimen SPS4 prematurely buckled due to the use of slender bracing system. The brace buckling caused the frame analysis to become a time-consuming process, and the analysis was therefore stopped.

The effect of stiffeners provided in the shear link web may be studied through comparing the performance of the specimens SPS5 and SPS6. These specimens behaved almost the same up to five times the drift corresponding to yielding. However, based on an experimental investigation, carried out at the Building and Housing Research Centre of Iran, the stiffeners play a key role in the shear panel behaviour at larger drifts. Observations indicate that shear panels with no stiffeners are susceptible to buckle severely at the imposed displacement more than five times yielding drift. Web local buckling in the shear panel adversely degrades the behaviour of the frame braced by SPS.

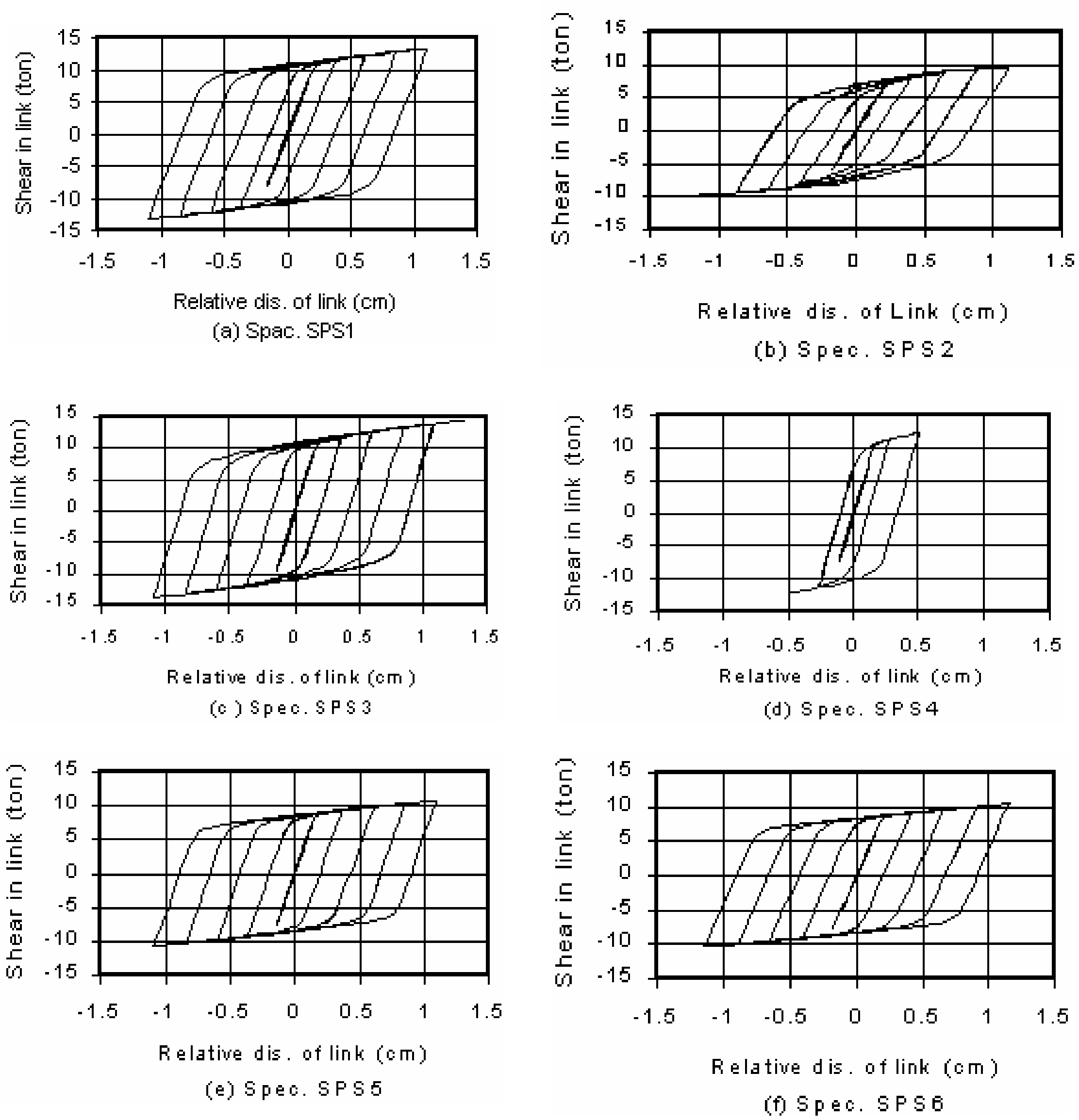

Figure 5. Shear force-relative displacement hysteretic response

5.1 Hysteretic response of shear panels

In Figure 5, the applied shear force on the link is drawn versus the corresponding shear deformation. Comparing Figs. 4 and 5, it is concluded that the shear panel has the main contribution to the cyclic behaviour of the whole frame, and the input energy is dominantly dissipated by the shear panel.

5.2 Dissipated energy

The shear link participation to the energy dissipation is shown in Figure 6. The figure shows that in each specimen more than 90 per cent of input energy was dissipated by the shear panel. The dissipated energy is considered as the plastic portion of the area surrounded by each hysteretic loop.

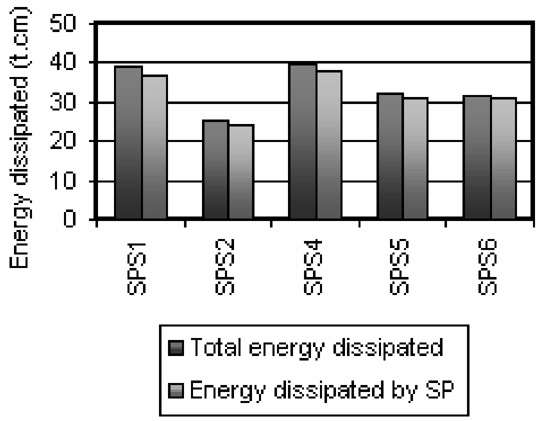

Figure 6. Energy dissipated by the whole frame and by the shear panel

The remaining portion of the input energy was dissipated within the panel zone at the intersection of the link and beam. Figure 7 illustrates a typical von Mises equivalent stress distribution near the link-to-beam intersection. The stress values shown in this figure is in kg/cm^2. The maximum equivalent stress is taken place within the shear panel with a magnitude of 2800 kg/cm^2, approximately.

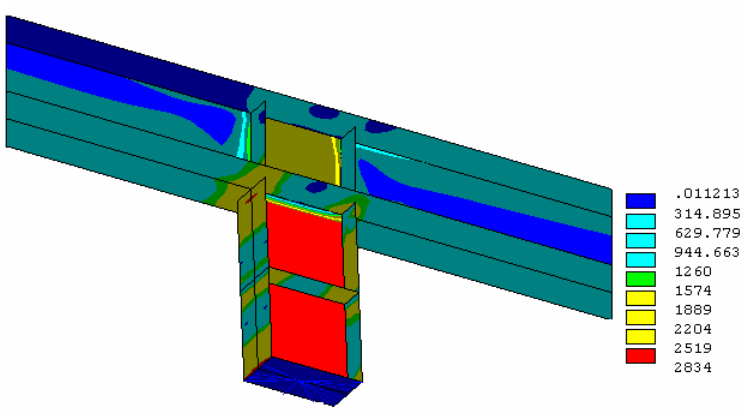

Figure 7. A typical von Mises equivalent stress contour

6. MATHEMATICAL MODEL FOR LATERAL STIFFNESS

Consider a moment frame braced by the shear panel system, as shown in Figure 8(a). Assuming that the braces can provide an extremely stiff region and considering the panel zone deformation details as shown in Figure 8(b), the frame may be modeled as illustrated in Figure 8(c).

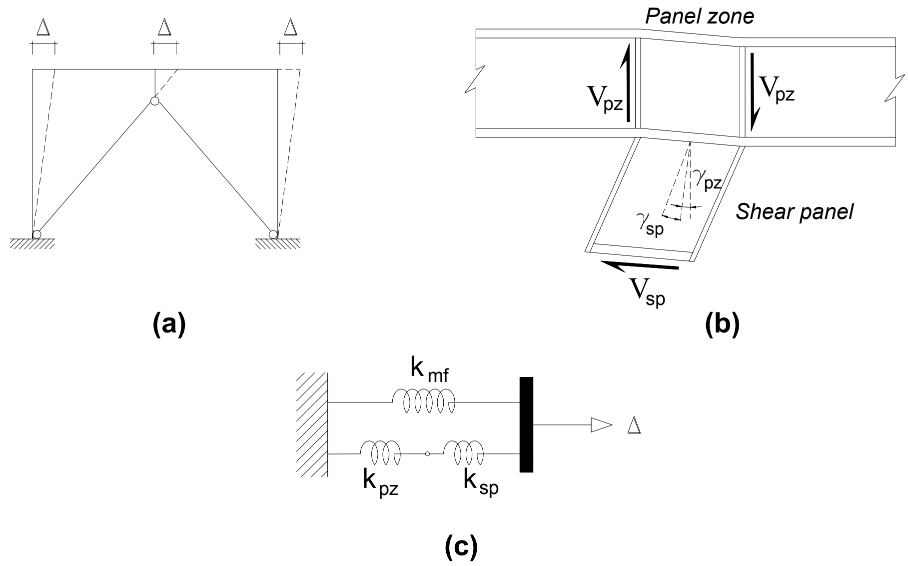

Figure 8. (a) Moment frame braced by shear panel system; (b) deformation of shear panel and beam panel zone in detail; (c) Equivalent spring model for the frame

The model consists of three springs: a set of two elasto-plastic springs in series, k_{pz} and k_{sp}, parallel to an elastic spring, k_{mf}. The parameters k_{pz} and k_{sp} denotes the stiffness of the beam panel zone and that of the shear panel, respectively. k_{mf} designates the moment frame stiffness. Since the moment frame is to remain elastic during lateral loading, the stiffness k_{mf} can readily be derived by the elastic analysis of the frame, as follow:

$$k_{mf} = \frac{12EI_c}{L_c^3}\left[\frac{I_c/L_c + 6I_b/L_b}{2I_c/L_c + 3I_b/L_b}\right] \tag{1}$$

in which E is Young's modulus; I_b and I_c are, respectively, the beam and column moment of inertia; L_b and L_c are the length of beam and column, respectively.

The stiffness of the shear panel may be evaluated by following expressions [16]:

$$k_{sp} = \frac{V_{sp}}{\delta_{sp}} = 0.95 d_{sp} t_{sp} G / L_{sp} \qquad \text{for} \quad 0 \le \gamma_{sp} \le \gamma_y$$

$$k_{sp} = \frac{dV_{sp}}{d\delta_{sp}} = 1.095\, b_{spf} t_{spf}^2 G / L_{sp}^2 \qquad \text{for} \quad \gamma_y \le \gamma \le 4\gamma_y \tag{2}$$

in which G, γ_{sp}, γ_y are the shear modulus, the shear panel distortion, and the shear distortion at general yielding, respectively. d_{sp}, t_{sp}, b_{spf}, and t_{spf} are web depth, web thickness, flange width and flange thickness of the shear panel, respectively. L_{sp} is the net length of the shear panel. For shear distortion greater than $4\gamma_y$, a constant strain hardening stiffness describes the shear panel performance. Since the shear distortion of the shear panel is usually much more than $4\gamma_y$ (γ_y equals 0.0017 for mild steel having $F_y = 2400\,kg/cm^2$), it is not irrational to take the shear panel stiffness as follow:

$$k_{sp} = \frac{dV_{sp}}{d\delta_{sp}} = 0.95 d_{sp} t_{sp} G_s / L_{sp} \tag{3}$$

where G_s is the tangent shear modulus and assumed to be $G/100$.

The same expressions as given in Eq. 2 can be employed for the stiffness of the beam panel zone shown in Figure 8(b). In such a case the parameters d_{sp}, t_{sp}, b_{spf}, t_{spf}, and L_{sp} are replaced with d_b, t_b, b_{bf}, t_{bf}, and d_{sp}, respectively. The parameters d_b, t_b, b_{bf}, and t_{bf} are web depth, web thickness, flange width and flange thickness of the beam panel zone, respectively. The numerical results show that the beam panel zone is partially yielded, but it can not develop a significant inelastic deformation. As a consequence, the stiffness of the beam panel zone is evaluated as:

$$k_{pz} = \frac{dV_{pz}}{d\delta_{pz}} = 1.095\, b_{bf} t_{bf}^2 G / d_{sp}^2 \tag{4}$$

The shear force acting on the beam panel zone, V_{pz}, is estimated as follows:

$$V_{pz} = L_{sp} V_{sp} \left[\frac{1}{0.95 d_{sp}} - \frac{L_{sp} + d_b/2}{L_{sp}} \cdot \frac{1}{L_b} \right] \tag{5}$$

Substituting Eq. 5 into Eq. 4, following equation yields:

$$k_{pz} = \frac{dV_{pz}}{d\delta_{pz}} = (1.095 b_{bf} t_{bf}^2 G / d_{sp}^2) / [L_{sp} / 0.95 d_{sp} - (L_{sp} + d_b/2)/L_b] \tag{6}$$

The energy dissipated by the whole frame also directly depends on the braced frame stiffness k_{bf}, which is obtained as:

$$k_{bf} = k_{mf} + \frac{1}{1/k_{sp} + 1/k_{pz}} \tag{7}$$

in which the parameters k_{mf}, k_{pz} and k_{sp} are calculated by Eqs. 1, 3 and 6, respectively.

In case that the beam is simply connected to the columns, the first term of the right hand in Eq. 7 can be omitted. Moreover, the stiffness of the beam panel zone is notably more than that of the shear panel. Hence, for a braced frame having simple beam-to-column connections, we have:

$$k_{bf} \approx k_{sp} = 0.95\, d_{sp}\, t_{sp}\, G_s / L_{sp} \tag{8}$$

and it is concluded that the whole energy dissipated can be expressed in terms of $d_{sp}t_{sp}/L_{sp}$.

In Figure 9, the relation between the energy dissipated and the braced frame stiffness according to the above expression, normalized by Young's modulus, is illustrated. The data correlates well with the trend-line depicted in the figure.

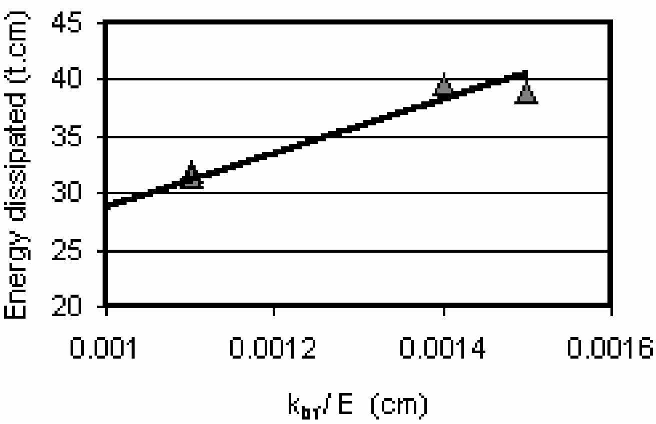

Figure 9. Relation between the energy dissipated and the braced frame stiffness

7. CONCLUSIONS

This paper dealt with the key issues influencing cyclic response of the braced frames using shear panel system. To this end, a number of single story-single bay frames were numerically analyzed using nonlinear finite element procedure. The main results are pointed out as follows:

1. Using shear panel bracing as a dual system significantly promotes the cyclic behaviour of the braced moment frame without notable reduction in the elastic lateral stiffness of the frame.

2. Choosing a shorter link as the shear panel, the adverse effect of the frame with simple connections can be reduced to some extent. The numerical results show that for the cases studied in this paper the use of shorter link increases energy dissipation capacity of the braced frame by 50 percent compared with the similar braced frame having longer link.
3. Web stiffeners provided in the shear panel, improve the behaviour of the shear panel and thus the braced frame, especially for larger deformations.
4. Considering drift limitations for the frame, the energy dissipation capability of the SPS can be improved by increasing the web depth and web thickness of the shear panel, or by reducing the shear panel length. The energy dissipated by the shear panel is linearly proportional to the parameter $d_{sp}t_{sp}/L_{sp}$.

Acknowledgment: The numerical work of this paper was conducted as part of a research project sponsored by the Building and Housing Research Centre of Iran through Grant No. 1-4560. Their support is gratefully acknowledged. The findings and opinions presented in this paper, however, are those of the authors, and not necessarily those of the sponsor.

REFERENCES

1. Popov, E.P. "Seismic behaviour of structural subassemblages", *J. Struct. Div.,* ASCE 1980, **106**(ST7), 1451-1474.
2. Engelhardt, M.D., and Husain, A.S. "Cyclic-loading performance of welded flange-bolted web connections", *J. Struct. Engng.*, AISC, No. 12, **119**(1993) 3537-3550.
3. Miller, D.K. "Lessons learned from the Northridge earthquake." *Engng. Struct.*, No. 4-6, **20**(1998) 249-260.
4. Mahin, S.A. "Lessons from damage to steel buildings during the Northridge earthquake." *Engng. Struct.*, No. 4-6, **20**(1998) 261-270.
5. Calado, L. "Cyclic behaviour of beam to column bare steel connection: Influence of column size", In: Mazzolani, editor, Moment resistant connections of steel frames in siesmic areas, E & FN SPON 2000, 267-290.
6. Roeder, C.W., and Popov, E.P. "Eccentrically braced steel frames for earthquaks", *J. Struct. Div.* ASCE 1978, **104**(ST7), 391-411.
7. Aristizabal-Ochao, J.D. "Disposable knee bracing: improvement in seismic design of steel frames", *J. Struct. Engng.*, ASCE, No. 7, **112**(1986) 1544-1552.
8. Balendra, T., Sam, M.T., and Liaw, C.Y. "Diagonal brace with ductile knee anchor for aseismic steel frame", *Earthquake Engng. Struct. Dyn.*, No. 6, **19**(1990) 847-858.
9. Balendra, T., Sam, M.T., and Liaw, C.Y. "Design of earthquake-resistant steel frames with knee bracing", *J. Construct. Steel Res.,* No. 3, **18**(1991) 193-208.
10. Sam, M.T., Balendra, T., and Liaw, C.Y. "Earthquake-resistant steel frames with energy dissipating knee elements", *Engng. Struct.*, No. 5, **17**(1995) 334-343.
11. American Institute of Steel Construction (AISC), *Seismic provisions for structural steel buildings*, Chicago, 1997.
12. Zahrai, S.M., and Bruneau, M. "Ductile end-diaphragm for seismic retrofit of slab-on-girder steel bridges", *J. Struct. Engng.*, ASCE, No. 1, **125**(1999), 71-80.

13. Zahrai, S.M., and Bruneau, M. “Cyclic testing of ductile end diaphragms slab-on-girder steel bridges”, *J. Struct. Engng.*, ASCE, No. 9, **125**(1999) 987-996.
14. ANSYS (Revision 5.4), User’s Manual, Theory, Swanson Analysis Systems, Inc., **4**(1992).
15. Engelhardt, M.D., and Popov, E.P. “Experimental performance of long links in eccentrically braced frames”, *J. Struct. Engng.*, ASCE, No. 11, **118**(1992) 3067-3088.
16. Krawinkler, H. “Shear in beam-column joints in seismic design of steel frames”, *Engng. J.*, AISC, No. 3, **15**(1978) 82-91.